Direct leptin action on POMC neurons regulates glucose homeostasis and hepatic insulin sensitivity in mice

Eric D. Berglund,[1] Claudia R. Vianna,[1] Jose Donato Jr.,[1] Mi Hwa Kim,[1] Jen-Chieh Chuang,[1] Charlotte E. Lee,[1] Danielle A. Lauzon,[1] Peagan Lin,[1] Laura J. Brule,[1] Michael M. Scott,[1] Roberto Coppari,[1] and Joel K. Elmquist[1,2]

[1]Division of Hypothalamic Research, Department of Internal Medicine, and [2]Department of Pharmacology, University of Texas Southwestern Medical School, Dallas, Texas, USA.

Leptin action on its receptor (LEPR) stimulates energy expenditure and reduces food intake, thereby lowering body weight. One leptin-sensitive target cell mediating these effects on energy balance is the proopiomelanocortin (POMC) neuron. Recent evidence suggests that the action of leptin on POMC neurons regulates glucose homeostasis independently of its effects on energy balance. Here, we have dissected the physiological impact of direct leptin action on POMC neurons using a mouse model in which endogenous LEPR expression was prevented by a *LoxP*-flanked transcription blocker (*lox*TB), but could be reactivated by Cre recombinase. Mice homozygous for the $Lepr^{loxTB}$ allele were obese and exhibited defects characteristic of LEPR deficiency. Reexpression of LEPR only in POMC neurons in the arcuate nucleus of the hypothalamus did not reduce food intake, but partially normalized energy expenditure and modestly reduced body weight. Despite the moderate effects on energy balance and independent of changes in body weight, restoring LEPR in POMC neurons normalized blood glucose and ameliorated hepatic insulin resistance, hyperglucagonemia, and dyslipidemia. Collectively, these results demonstrate that direct leptin action on POMC neurons does not reduce food intake, but is sufficient to normalize glucose and glucagon levels in mice otherwise lacking LEPR.

Introduction

Leptin is an adipose-derived hormone that acts on its cognate receptors (LEPR) expressed by multiple neuronal groups in distinct areas of the brain (1). The canonical effect of leptin action in the brain is to regulate food intake and energy expenditure and thus body weight (2–4). In addition, leptin regulates several other physiological processes, including hepatic glucose production, insulin action, and glucagon levels (5–10). It is still unclear, however, which neurons mediate the varied physiological effects of leptin.

One population of neurons targeted by leptin is proopiomelanocortin (POMC) cells in the arcuate nucleus of the hypothalamus (ARH) and nucleus of the solitary tract (NTS) (2, 3). Leptin action on POMC neurons in the ARH is considered a prototypical site of action in the control of energy balance. This view is partly based on results showing that loss of LEPR in POMC neurons increases body weight (8, 11, 12). Conversely, LEPR reexpression in the ARH (13), overexpression in the ARH (14–17), and transgenic expression in POMC neurons (18) lower body weight. Interestingly, these latter studies also show lowered blood glucose, suggesting that leptin-sensitive POMC neurons in the ARH directly modulate metabolism (13–18). In the current study, we developed what we believe to be a novel LEPR-null mouse model in which endogenous LEPR expression can be reexpressed in cells that normally express leptin receptors. Here, we reexpress LEPR only in POMC neurons to delineate the physiological effects on energy and metabolic homeostasis.

Authorship note: Eric D. Berglund and Claudia R. Vianna are co–first authors.

Conflict of interest: The authors have declared that no conflict of interest exists.

Citation for this article: *J Clin Invest.* 2012;122(3):1000–1009. doi:10.1172/JCI59816.

Results

Development and validation of the Lepr reactivatable mouse model. Similarly to work in previous studies (19–23), a *LoxP*-flanked transcription-blocking cassette was inserted between exons 16 and 17 of the *Lepr* gene to generate mice lacking the long (B) isoform (Supplemental Figure 1A; supplemental material available online with this article; doi:10.1172/JCI59816DS1). As predicted, $Lepr^{loxTB/loxTB}$ ($Lepr^{loxTB}$) mice were obese compared with $Lepr^{WT/WT}$ (WT) controls and comparable to mice harboring naturally occurring LEPR mutations (e.g. *db/db*; ref. 24 and data not shown). $Lepr^{loxTB}$ mice were also hyperglycemic, similarly to *db/db* animals (data not shown). As a first test of the utility of this model, we made mice with global reexpression of LEPR (Figure 1B). To do so, male $Lepr^{loxTB/WT}$ mice were first bred with female $Lepr^{loxTB/WT}$ mice, which express zona pellucida 3-*cre* (Zp3-*cre*) (25). The genotypes of resulting progeny were produced at expected Mendelian ratios (data not shown). Restoration of LEPR expression in $Lepr^{loxTB}$ × Zp3-*cre* mice rescued obesity and hyperglycemia to levels comparable to that in WT controls, demonstrating that the *cre*-reactivated $Lepr^{loxTB}$ allele was functional (data not shown).

Next, $Lepr^{loxTB/WT}$ mice were bred with $Lepr^{loxTB/WT}$ × POMC-*cre* mice (11) to restore expression of the B isoforms of LEPR in POMC neurons. Genotypes of resulting progeny were produced at expected Mendelian ratios. Expression of functional LEPR in POMC neurons was validated based on leptin-stimulated phosphorylation of Stat3 (p-Stat3) immunoreactivity in brains of fasted mice. As expected, leptin increased p-Stat3 in numerous regions of the hypothalamus in WT mice (Figure 1A). In contrast, leptin-induced p-Stat3 immunoreactivity was completely absent in $Lepr^{loxTB}$ littermates (Figure 1B). In $Lepr^{loxTB}$ × POMC-*cre* mice, leptin-stimulated p-Stat3 was detectable only in the ARH, indicating reexpression

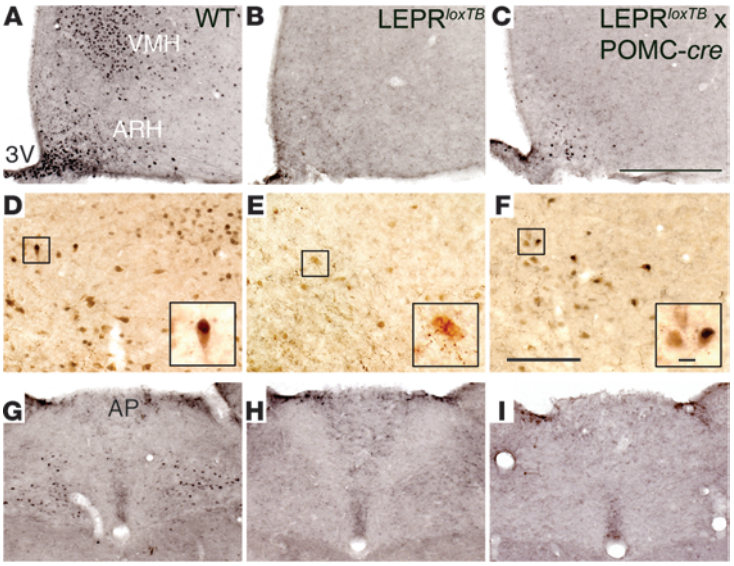

Figure 1
LEPRs are only reactivated in the ARH in *Lepr*^{loxTB} × POMC-*cre* mice. Representative images of leptin-stimulated (5 mg/kg body weight; i.p.) increases in phosphorylation of Stat3 (p-Stat3) immunoreactivity in 18-hour–fasted, 8-week-old, male WT, LEPR-null mice generated by inserting floxed transcription blocking sequences in the LEPR gene (*Lepr*^{loxTB}) and mice in which LEPRs are selectively reactivated in POMC neurons (*Lepr*^{loxTB} × POMC-*cre*). Hypothalamus is shown in **A**–**C**. Double immunohistochemistry for p-Stat3 (black) and β-endorphin (brown) is shown in **D**–**F**. Insets in **D**–**F** show increased magnification of cells, if any, which overlap. Hindbrain is shown in **G**–**I**. 3v, third ventricle; VMH, ventromedial hypothalamus; AP, area postrema. n = 8–10 for p-Stat3; n = 3 for β-endorphin. Scale bars: 400 μm (**C**); 200 μm (**F**); 10 μm (**F**, inset).

of LEPR in POMC neurons (Figure 1C). Costaining p-Stat3–positive neurons in the ARH of WT and *Lepr*^{loxTB} × POMC-*cre* mice for β-endorphin indicated that approximately one-third of cells overlapped (Figure 1, D and F). There was no overlap between p-Stat3 and β-endorphin in the ARH of *Lepr*^{loxTB} littermates (Figure 1E).

To investigate whether LEPR expression is reactivated in POMC neurons outside the ARH, leptin-stimulated p-Stat3 immunoreactivity was also assessed in the hindbrain. Leptin activated p-Stat3 in the hindbrain of WT mice (Figure 1G). This effect was absent in *Lepr*^{loxTB} and *Lepr*^{loxTB} × POMC-*cre* mice (Figure 1, H and I). In addition, immunohistochemistry was used to label ACTH-producing cells in the pituitary of LEPR-*cre* × tdTomato mice. These results show that few cells in the pituitary coexpress LEPR and ACTH (Supplemental Figure 2, A–C). Plasma corticosterone levels were also similar in 5-hour–fasted *Lepr*^{loxTB} and *Lepr*^{loxTB} × POMC-*cre* mice (292 ± 53 and 293 ± 48, respectively). Collectively, these results demonstrate that *Lepr*^{loxTB} × POMC-*cre* mice only express functional LEPR in POMC neurons in the ARH and that our genetic strategy to reactivate this pathway occurs in a physiological manner.

Leptin action in POMC neurons stimulates energy expenditure, but does not regulate food intake. To determine whether LEPR reactivation in POMC neurons is sufficient to rescue obesity and hyperphagia characteristic of LEPR-null mice, we assessed body weight/composition and energy balance. As shown in Figure 2A, male *Lepr*^{loxTB} and *Lepr*^{loxTB} × POMC-*cre* littermates were similarly obese from 4–12 weeks. Body weight in male *Lepr*^{loxTB} × POMC-*cre* mice then diverged after 12 weeks versus *Lepr*^{loxTB} littermates and was approximately 15% lower at 20 weeks (Figure 2A). The magnitude of this effect is noteworthy, as it mirrors weight gain ascribed to deletion of LEPR in POMC neurons in the ARH (11). Decreased fat mass in male *Lepr*^{loxTB} × POMC-*cre* mice compared with *Lepr*^{loxTB} littermates fully accounted for lowered body weight after 12 weeks (Figure 2B). There were no differences in lean mass between male *Lepr*^{loxTB} mice and *Lepr*^{loxTB} × POMC-*cre* littermates (Figure 2C). Female *Lepr*^{loxTB} × POMC-*cre* mice were also comparably obese to *Lepr*^{loxTB} littermates, but this effect did not vary with age (Figure 2D). There were no differences in body weight or composition between WT and LEPR$^{WT/WT}$ × POMC-*cre* mice, indicating that expression of *cre*-recombinase in POMC neurons did not independently have an impact on energy balance (Figure 2, A–D).

To examine leptin's impact on energy balance and determine mechanism or mechanisms by which LEPR reactivation in POMC neurons reduces body weight in male mice, we used metabolic cages to measure energy expenditure and food intake. Importantly, this was done in *Lepr*^{loxTB} and *Lepr*^{loxTB} × POMC-*cre* littermates with similar body weight/composition, which are obese compared with WT controls (Figure 3A). Oxygen consumption and carbon dioxide production expressed relative to total body weight were reduced in *Lepr*^{loxTB} mice compared with WT controls, but were partially restored compared with *Lepr*^{loxTB} × POMC-*cre* littermates (Figure 3, B and C). The respiratory exchange ratio (RER) was lower in *Lepr*^{loxTB} mice than in WT controls, but was increased in *Lepr*^{loxTB} × POMC-*cre* littermates compared with all groups (Figure 3D). Total activity was reduced in *Lepr*^{loxTB} mice compared with WT controls, but was increased over a 24-hour period and during the dark cycle in *Lepr*^{loxTB} × POMC-*cre* mice compared with other groups (Figure 3E). In contrast, food consumption was similarly elevated in *Lepr*^{loxTB} and *Lepr*^{loxTB} × POMC-*cre* mice versus WT controls (Figure 3F). Collectively, these results demonstrate that LEPR direct leptin action in POMC neurons in the ARH regulates energy expenditure, but not food intake.

Leptin action in POMC neurons normalizes glucose and glucagon levels and improves hepatic insulin sensitivity. We next assessed the impact of direct leptin action on POMC neurons on several parameters of glucose homeostasis. As expected, blood glucose in male *Lepr*^{loxTB} mice was elevated versus that in WT controls (Figure 4A). Despite only modest effects on body weight and adiposity, blood glucose in male *Lepr*^{loxTB} × POMC-*cre* mice was fully normalized to WT levels at all measured time points (Figure 4A). Normalization of blood glucose in male *Lepr*^{loxTB} × POMC-*cre* mice was evident at 6, 8, and 12 weeks, which was prior to divergence of body weight (Figure 4A and Figure 2A). This indicates that this effect is independent of changes in body weight or adiposity. Plasma insulin in male *Lepr*^{loxTB} × POMC-*cre* mice was lowered compared with *Lepr*^{loxTB} littermates at 8 weeks, but this difference was absent at 12 and 20 weeks (Figure 4B). Blood glucose and plasma insulin were also similarly lowered in female *Lepr*^{loxTB} × POMC-*cre* mice in weight- and body composition–matched littermates (Figure 4, C and D). Leptin was similarly elevated in *Lepr*^{loxTB} and *Lepr*^{loxTB} × POMC-*cre* mice at 12 and

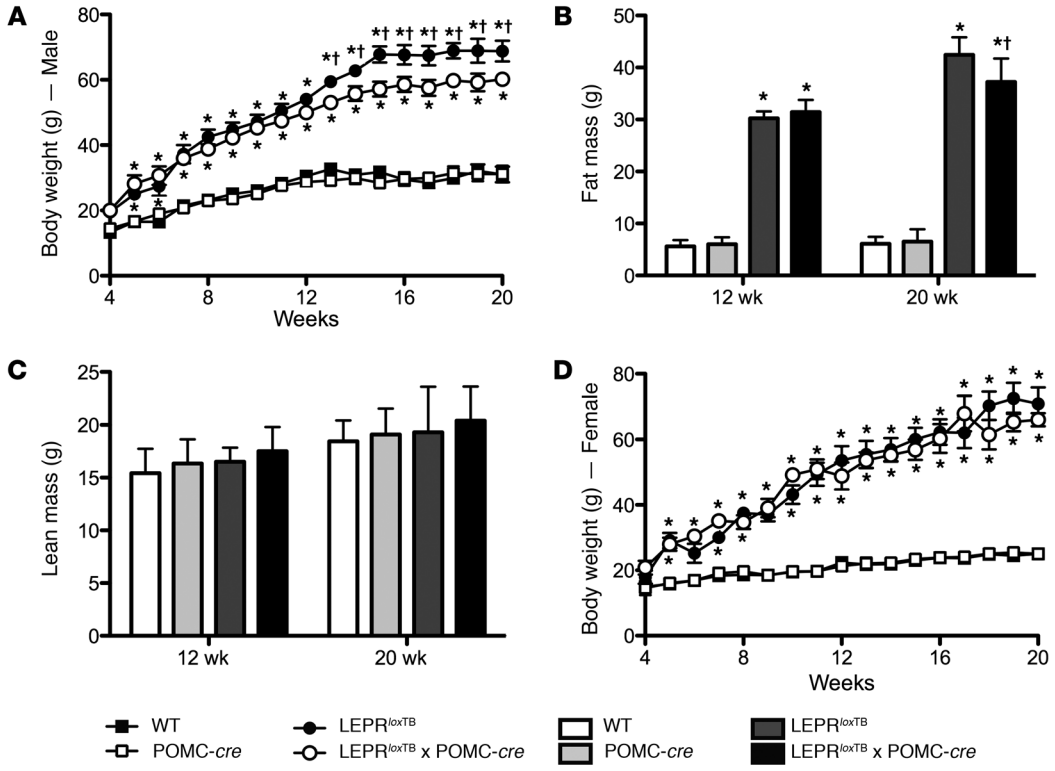

Figure 2
Body weight is modestly reduced only in male *Lepr*^{loxTB} × POMC-*cre* mice after 12 weeks of age compared with *Lepr*^{loxTB} littermates. Body weight and composition in WT, WT expressing *Cre*-recombinase in POMC neurons, LEPR-null mice generated by inserting floxed transcription blocking sequences in the *Lepr* gene (*Lepr*^{loxTB}), and littermates in which LEPRs are selectively reactivated in POMC neurons (*Lepr*^{loxTB} × POMC-*cre*). Body weight in male and female mice is shown in **A** and **D**. Fat and lean mass assessed by NMR in male mice at 12 and 20 weeks are shown in **B** and **C**. **P* < 0.05; †*P* < 0.05 versus WT controls and *Lepr*^{loxTB}, respectively. *n* = 12–15 and 7–9 for male and female mice, respectively. Data are presented as mean ± SEM.

20 weeks compared with levels in WT controls (Figure 4E). There were also no differences in blood glucose, plasma insulin, or plasma leptin between WT and LEPR$^{WT/WT}$ × POMC-*cre* mice, indicating that expression of *Cre*-recombinase in POMC neurons did not independently alter these parameters (Figure 4, A–E). Collectively, these results demonstrate that LEPR signaling only in POMC neurons in the ARH potently regulates blood glucose levels.

We next explored potential mechanisms underlying the ability of leptin action on POMC neurons to regulate blood glucose levels. We used tracer dilution and hyperinsulinemic-euglycemic clamp techniques in 4- to 5-hour–fasted, conscious, chronically catheterized 8-week-old male mice to investigate changes in glucose flux and to determine whether and where insulin action is improved by LEPR reexpression in POMC neurons. Body weight–matched cohorts of *Lepr*^{loxTB} and *Lepr*^{loxTB} × POMC-*cre* littermate mice were used (Figure 5A). Blood glucose levels were clamped at target levels in all mice (Figure 5B). The steady-state glucose infusion rate (GIR) required to clamp blood glucose in *Lepr*^{loxTB} × POMC-*cre* mice was increased 150% compared with *Lepr*^{loxTB} littermates, indicating improved whole-body insulin sensitivity (Figure 5C). Clamp insulin levels were similar between *Lepr*^{loxTB} and *Lepr*^{loxTB} × POMC-*cre* mice, indicating that this variable did not contribute to differences in GIR (Figure 5D). Consistent with lowered short-term fasted blood glucose levels in *Lepr*^{loxTB} × POMC-*cre* mice, basal glucose turnover was reduced versus that in *Lepr*^{loxTB} animals (Figure 5E). During the clamp, insulin-stimulated suppression of endogenous rate of glucose appearance (endoR_a) was restored to WT levels in *Lepr*^{loxTB} × POMC-*cre* mice (Figure 5E). *Lepr*^{loxTB} mice displayed expected defects in hepatic insulin sensitivity (Figure 5E). In contrast to marked improvements in the liver, insulin-stimulated glucose disposal was similarly impaired in both *Lepr*^{loxTB} and *Lepr*^{loxTB} × POMC-*cre* mice compared with WT controls (Figure 5F). This suggests that reexpression of LEPRs only in POMC neurons improves insulin sensitivity in the liver, but not in other insulin target tissues such as skeletal muscle and adipose tissue.

We also assessed plasma glucagon levels in all groups of mice. We found that glucagon was elevated in male *Lepr*^{loxTB} mice at 12 and 20 weeks, but fully restored to WT levels in *Lepr*^{loxTB} × POMC-*cre* littermates (Figure 6A). Plasma glucagon levels were also inappropriately regulated in response to a fasting/refeeding paradigm in *Lepr*^{loxTB} mice. Glucagon was elevated in *Lepr*^{loxTB} mice in the fed, fasted, and carbohydrate-refed condition (Figure 6B). In contrast, plasma glucagon levels in *Lepr*^{loxTB} × POMC-*cre* mice were lowered to WT control levels in the fed and carbohydrate-refed state (Figure 6B). Plasma insulin levels in carbohydrate-refed *Lepr*^{loxTB} × POMC-*cre* mice were also reduced compared with those in *Lepr*^{loxTB} animals (Figure 6C). Pancreata were also isolated to determine whether glucagon and/or insulin content differ in *Lepr*^{loxTB} × POMC-*cre* mice compared with *Lepr*^{loxTB} littermates.

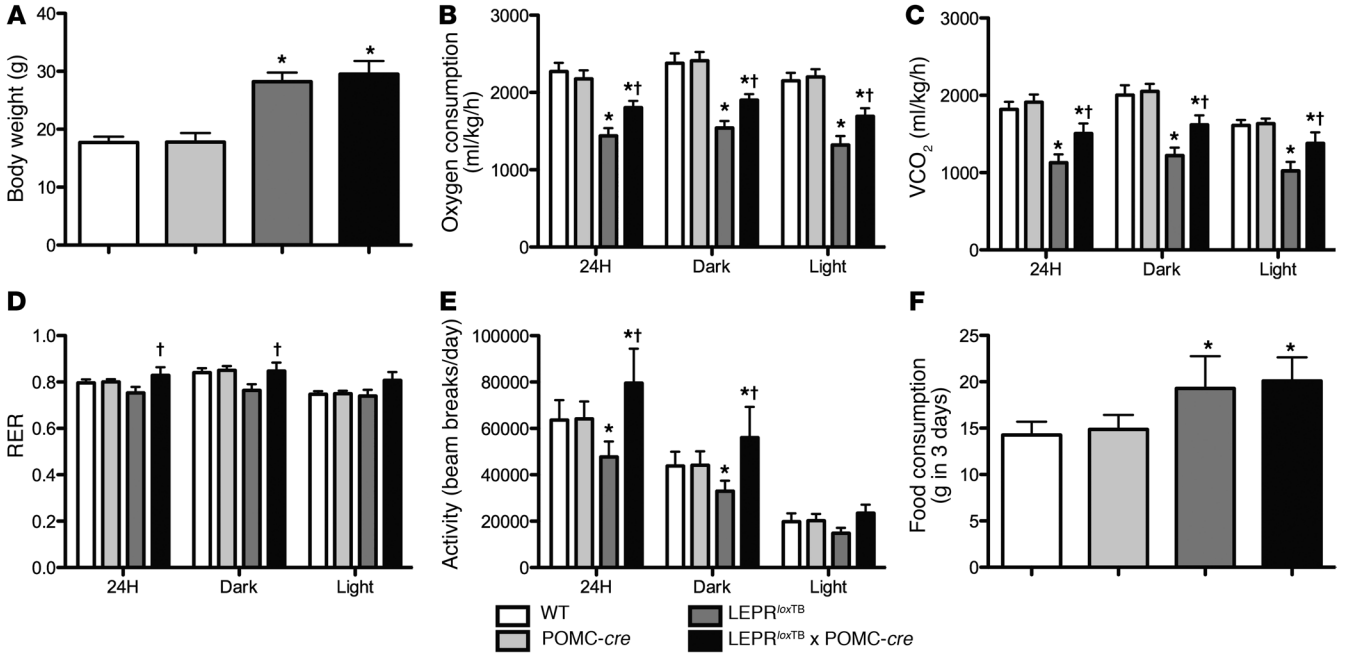

Figure 3

Selective reactivation of LEPR expression in POMC neurons stimulates increased energy expenditure, but does not affect food intake in mice. Metabolic cage studies in male, 6-week-old WT, WT expressing Cre-recombinase in POMC neurons, LEPR-null mice generated by inserting floxed transcription blocking sequences in the *Lepr* gene (*Lepr*^{loxTB}), and littermates in which LEPRs are selectively reactivated in POMC neurons (*Lepr*^{loxTB} × POMC-*cre*) assessed using TSE Metabolic Cages. Body weight is shown in **A**. Oxygen consumption, carbon dioxide production, RER, total activity, and food consumption normalized to total body weight are shown in **B**–**F**, respectively. *$P < 0.05$; †$P < 0.05$ versus WT controls and *Lepr*^{loxTB} mice, respectively. n = 7–10 mice/genotype. Data are presented as mean ± SEM.

We found that pancreatic content of both hormones was similarly elevated above that in WT controls in *Lepr*^{loxTB} × POMC-*cre* and *Lepr*^{loxTB} littermate mice (Figure 6, D and E).

The contribution of normalized plasma glucagon in *Lepr*^{loxTB} × POMC-*cre* mice to improvements in insulin sensitivity based on GIR (Figure 5C) and suppression of endoR_a (Figure 5E) was next examined. To test this, somatostatin was infused at the onset of the clamp to acutely suppress endogenous glucagon and insulin secretion in *Lepr*^{loxTB} × POMC-*cre* and *Lepr*^{loxTB} littermate mice of similar body weights (41.9 ± 1.2 and 40.8 ± 1.4 g, respectively). Blood glucose was clamped at target levels in both groups (Figure 6F). The GIR required to clamp blood glucose was 113% higher in *Lepr*^{loxTB} × POMC-*cre* mice than *Lepr*^{loxTB} littermates, indicating higher insulin sensitivity (Figure 6G). Importantly, this occurred despite no differences in glucagon or insulin between the 2 groups during clamp steady-state conditions (Figure 6, H and I, respectively). Plasma C-peptide was also lowered in both groups, indicating that somatostatin inhibited endogenous insulin secretion (basal levels were 11.6 ± 1.3 and 10.5 ± 0.6 ng/ml in *Lepr*^{loxTB} and *Lepr*^{loxTB} × POMC-*cre* mice, respectively, and were lowered to 0.7 ± 0.2 and 0.7 ± 0.1 ng/ml). In agreement with clamp results in Figure 5, E and F, the clamp-induced rise in insulin was more effective to suppress endoR_a in *Lepr*^{loxTB} × POMC-*cre* mice than *Lepr*^{loxTB} littermates (Figure 6J). Additionally, insulin-stimulated rate of glucose disappearance (R_d) was comparable between groups (Figure 6K).

Since glucose and lipid metabolism in the liver are interconnected and hormone action in the CNS is increasingly appreciated to regulate hepatic lipid metabolism (26, 27), we assessed plasma and hepatic triglycerides (TGs) and cholesterol in 12- and 20-week-old mice. Remarkably, plasma TG and cholesterol in *Lepr*^{loxTB} × POMC-cre mice were fully and partially restored, respectively, to WT control levels at both ages. (Figure 7, A and B). Hepatic TG was also lowered in *Lepr*^{loxTB} × POMC-*cre* mice to WT levels at both ages, but there were no changes in hepatic cholesterol (Figure 7, C and D). These data indicate that leptin action on POMC neurons in the ARH improves both the plasma and hepatic lipid profiles.

Discussion

In the current study, we tested the physiological impact of LEPR signaling in POMC neurons on energy balance, glucose, and lipid homeostasis. To do so, we generated a mouse model in which LEPRs are reexpressed only in the subset of POMC neurons that endogenously express LEPRs. We found that selective expression of LEPR in POMC neurons in the ARH on an otherwise LEPR-null background is sufficient to normalize blood glucose and plasma glucagon levels. This manipulation also improved hepatic insulin sensitivity as well as the plasma and hepatic lipid profile. Importantly, these effects were not secondary to reductions in body weight, adiposity, or food intake. Our data further reveal that leptin action on POMC neurons only modestly rescues the obesity characteristic of LEPR deficiency. This reduction in body weight was due to increased energy expenditure and not due to suppression of food intake. Interestingly, reductions in body weight and adiposity only occurred in male mice. Female mice did not exhibit any improvements in body weight, thus complementing prior evidence demonstrating sexually dimorphic LEPR-mediated regulation of energy balance via POMC neurons (28).

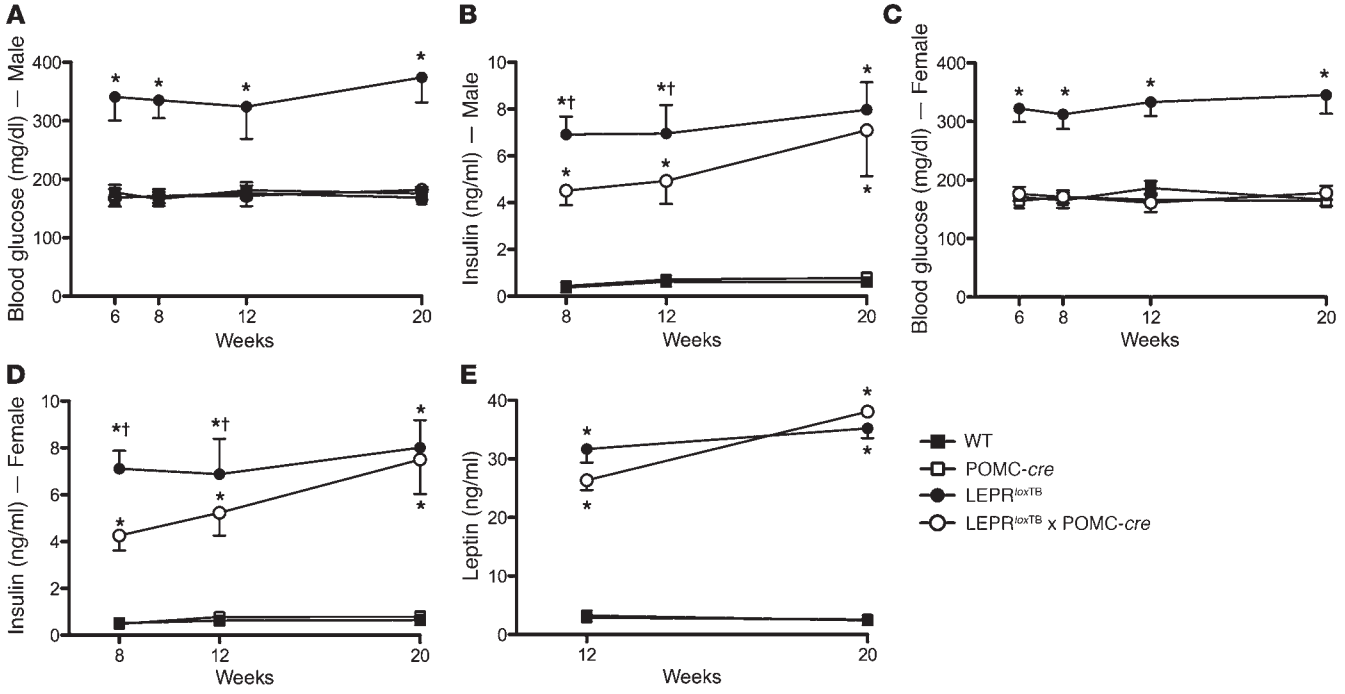

Figure 4
Selective reactivation of LEPR expression in POMC neurons improves hyperglycemia and hyperinsulinemia in mice. Blood glucose and plasma insulin in 5-hour–fasted male and female mice at various ages are shown in **A**–**D**. Plasma leptin in 24-hour–fasted male mice is shown in **E**. *$P < 0.05$; †$P < 0.05$ versus WT controls and *Lepr*^{loxTB} mice, respectively. n = 8–10 mice/genotype. Data are presented as mean ± SEM.

Previous work has shown that reactivation or overexpression of LEPR in neurons within the ARH lowers blood glucose levels (13–17). A caveat regarding these studies is that they were unable to identify specific neurons transducing leptin signals into normal glucose balance. Huo et al. (18) recently addressed this question using *cre*-dependent reexpression of LEPR in all POMC neurons in a *db/db* background. These authors found that transgenic expression of LEPR in all POMC neurons reduced body weight via effects on both energy expenditure and food intake and also lowered blood glucose and plasma insulin levels (18). The effects of reducing food intake in this model contrast with our results as well as our prior work in mice lacking LEPR in POMC neurons, where this loss had minimal effects on food intake in chow-fed mice (8, 11, 12). These disparate results are likely due to differences in the mouse models being examined. One possibility is that Huo et al. (18) used a CMV promoter to reexpress LEPR in POMC neurons, which resulted in transgenic overexpression of LEPR. The CMV promoter is also expressed by all POMC neurons that express *cre*-recombinase. Prior work has shown that *cre*-recombinase is present in approximately 95% of POMC neurons in the ARH (11), but only approximately 30%–40% express LEPR (29). We suggest that effects on food intake in Huo et al. (18) may be due to expression of LEPR in POMC neurons that do not normally express LEPR. Candidates for this effect are POMC neurons that express insulin or serotonin 2C receptors. Recent studies, for example, identify that serotonin 2C receptors in POMC neurons regulate food intake (21, 22). The current strategy to reactivate the endogenous receptor and in a physiological manner is supported by data showing that approximately 30%–40% of the p-Stat3–positive cells in the ARH coexpress β-endorphin.

Our results also demonstrate that direct leptin action on POMC neurons lowers glucagon levels and improves hepatic insulin sensitivity. Glucagon and insulin are fundamental to the control of glucose homeostasis, and defects in their regulation are hallmarks of type 2 diabetes (30). The current data related to glucagon complement recent work in models of uncontrolled or type 1 diabetes showing that leptin action in the brain improves glucose homeostasis, in part, by reducing levels of glucagon (5, 7, 31). These data also support pharmacological results in contexts of obesity and type 2 diabetes, finding that inhibition of hepatic glucagon action lowers blood glucose independently of any improvement in body weight and/or energy balance (32, 33). The current results using hyperinsulinemic-euglycemic clamps with or without somatostatin suggest that lowered plasma glucagon in *Lepr*^{loxTB} × POMC-*cre* accounts for some, but not all, of the improved ability of insulin to suppress endogenous glucose production. These data agree with work in rats showing that i.c.v. administration of leptin during a hyperinsulinemic-euglycemic clamp plus somatostatin enhances the ability of insulin to inhibit hepatic glucose production (34, 35). It is unclear whether lowered glucagon explains these prior results ascribed to leptin action in the CNS because glucagon levels were not reported (34, 35). An additional finding from the clamp studies is that reactivation of LEPR only in POMC neurons in the ARH does not have an impact on insulin-stimulated glucose disposal. This is of note because numerous studies have reported that central administration of leptin stimulates insulin-stimulated (36, 37) and non–insulin-stimulated (9, 38, 39) skeletal muscle glucose uptake. It is speculated that unidentified leptin-sensitive neurons outside the ARH are responsible for these effects.

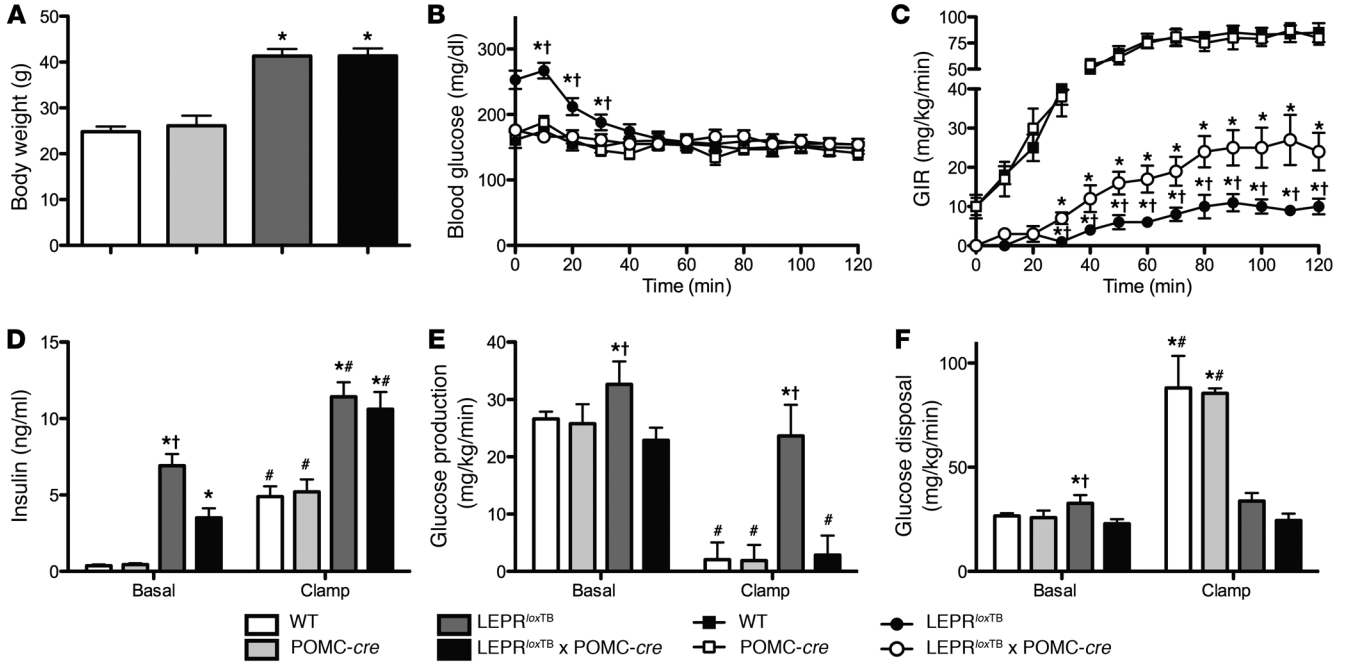

Figure 5

Selective reactivation of LEPR expression in POMC neurons improves hepatic insulin sensitivity in mice. Hyperinsulinemic-euglycemic (10 mU/kg/min, 150 mg/dl, respectively) clamps of 120 minutes in conscious, chronically catheterized, 4- to 5-hour–fasted, 8-week-old male WT, WT expressing *Cre*-recombinase in POMC neurons, LEPR-null mice generated by inserting floxed transcription blocking sequences in the *Lepr* gene ($Lepr^{loxTB}$), and littermates in which LEPRs are selectively reactivated in POMC neurons ($Lepr^{loxTB}$ × POMC-*cre*). Body weight on day of experiment is shown in **A**. Basal and clamp blood glucose, GIR, and plasma insulin are shown in **B**–**D**, respectively. Basal and insulin-stimulated (clamp steady-state [t = 80–120 minutes]) glucose production and disposal determined using [3-^{3}H]glucose are shown in **E** and **F**. Blood samples were taken from the cut tail. $^*P < 0.05$; $^\dagger P < 0.05$ versus WT controls and $Lepr^{loxTB}$ × POMC-cre mice, respectively; $^\#P < 0.05$ comparing basal to clamp values within a genotype. Data are presented as mean ± SEM.

An additional intriguing metabolic consequence of selective reactivation of LEPR on POMC neurons is marked improvements in circulating and hepatic TG and cholesterol levels. These findings are consistent with reports showing that leptin infusion in the brain of *ob/ob* mice regulates hepatic lipid metabolism, including plasma and liver TG and cholesterol (40–45). Our data suggest that leptin action on POMC neurons is one site where this regulation occurs. Moreover, these current data suggest that such effects can occur independently of leptin-mediated weight loss, which is an issue highlighted by others (44). These findings are potentially important because dyslipidemia and fatty liver are components of metabolic syndrome. It is interesting that these improvements persist in 20-week-old male $Lepr^{loxTB}$ × POMC-*cre* mice in which plasma insulin levels are as high as in LEPR-null littermates. This finding suggests that the regulatory impact of direct leptin action on POMC neurons in the ARH to ameliorate plasma dyslipidemia and hepatic TG accumulation is at least partially insulin independent. Lowered TG in the liver of $Lepr^{loxTB}$ × POMC-*cre* mice is also a possible contributor to improved hepatic insulin sensitivity and thus blood glucose levels. Several studies indicate a link between liver lipid content and hepatic insulin resistance (46–48). However, other studies conclude that elevated liver fat per se does not impair hepatic insulin sensitivity (49, 50). With these current data, it is important to consider that hepatic TGs are lowered in $Lepr^{loxTB}$ × POMC-*cre* mice versus $Lepr^{loxTB}$ littermates, but they are not normalized to WT levels. Additional work is needed to clarify whether $Lepr^{loxTB}$ × POMC-*cre* mice exhibit subtle differences in the type(s) of lipid present in the liver that may affect hepatic insulin sensitivity or whether these differences are unrelated.

It is currently unclear exactly how leptin action in POMC neurons within the ARH provokes these positive effects in contexts of obesity, hyperglycemia, and insulin resistance. We speculate that this pathway includes activation of melanocortin 4 receptor (MC4R; a target of POMC-derived α-MSH) signaling in the sympathetic nervous system (SNS) to regulate pancreas and liver. This notion is partly based on work showing that reactivation of MC4R in the SNS, but not the parasympathetic nervous system (PNS), of an otherwise MC4R-null mouse ameliorates hepatic insulin resistance. Numerous other reports also show that leptin acts in the brain to regulate the SNS (9, 51–53). However, other studies show that leptin acts via the PNS to mediate its beneficial effects (6, 36, 54). Additionally, leptin has been also shown to act independently of melanocortin signaling to modulate liver glucose metabolism. This is a complex issue, and additional studies are needed to test these various possibilities. An additional point in the current studies is that the genetic modification occurred prenatally, which may allow for plasticity and developmental compensation. This issue has been highlighted by work finding disparate phenotypes in mice with pre- and postnatal ablation of AgRP neurons (55). Recent studies have also reported that multiple lineages of hypothalamic neurons express POMC, including cells that do

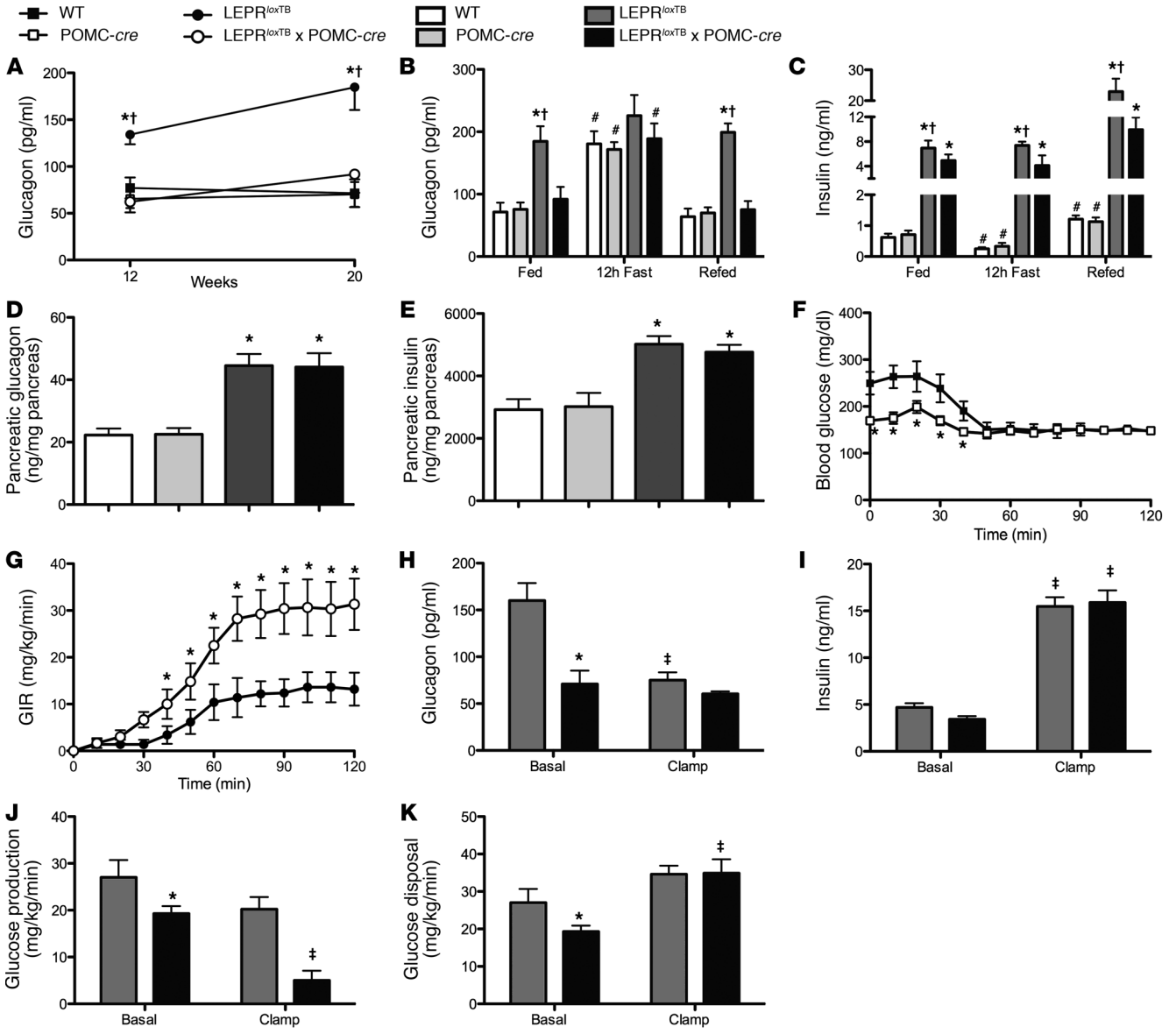

Figure 6

Inappropriate plasma glucagon levels are corrected in *Lepr*^{loxTB} × POMC-*cre* mice, and this contributes to improvements in hepatic insulin action. (**A**) Shown are body weight and 12-hour–fasted/carbohydrate-refed plasma glucagon (**B**) as well as insulin (**C**) in WT, WT expressing *Cre*-recombinase in POMC neurons, leptin receptor LEPR-null mice generated by inserting floxed transcription blocking sequences in the *Lepr* gene (*Lepr*^{loxTB}), and littermates in which LEPRs are selectively reactivated in POMC neurons (*Lepr*^{loxTB} × POMC-*cre*) (n = 8–10 mice/genotype). (**D** and **E**) Pancreatic glucagon and insulin content, respectively (n = 12–15 mice/genotype). (**F**) Blood glucose during 120-minute hyperinsulinemic-euglycemic (25 mU/kg/min, 150 mg/dl, respectively) clamps plus somatostatin (9 ng/kg/min) in conscious, chronically catheterized, 4- to 5-hour–fasted, 8- to 9-week-old male mice (n = 6 mice/genotype). (**G**) GIR is shown. (**H** and **I**) Basal and clamp plasma glucagon and insulin, respectively, are shown. (**J** and **K**) Basal and insulin-stimulated (clamp steady-state [t = 80–120 minutes]) glucose production and disposal determined using [3-^{3}H]glucose are shown. $^*P < 0.05$, comparing *Lepr*^{loxTB} to *Lepr*^{loxTB} × POMC-*cre* mice; $^\dagger P < 0.05$, comparing WT controls to *Lepr*^{loxTB} mice; $^\#P < 0.05$ comparing fed and refed mice; $^\ddagger P < 0.05$, comparing clamp to basal with a genotype. Data are presented as mean ± SEM.

not express POMC in adult mice (56). Future studies employing an inducible model of *cre*-recombinase in POMC neurons in the *Lepr*^{loxTB} mouse are needed to examine these issues.

In summary, leptin action on POMC neurons in the ARH exerts potent effects to regulate blood glucose levels. Our data also suggest that direct leptin action on POMC neurons does not underlie the ability of leptin to suppress food intake. These results support views that leptin action outside the ARH is needed to induce dramatic weight loss (57). In contrast, our results do not support the conventional model in which leptin acts on POMC in the ARH to simultaneously stimulate energy expenditure and suppress food intake (2, 3). Instead, our data support a modified model of direct leptin action on POMC neurons in the ARH to exert potent effects to regulate numerous facets of glucose homeostasis, including

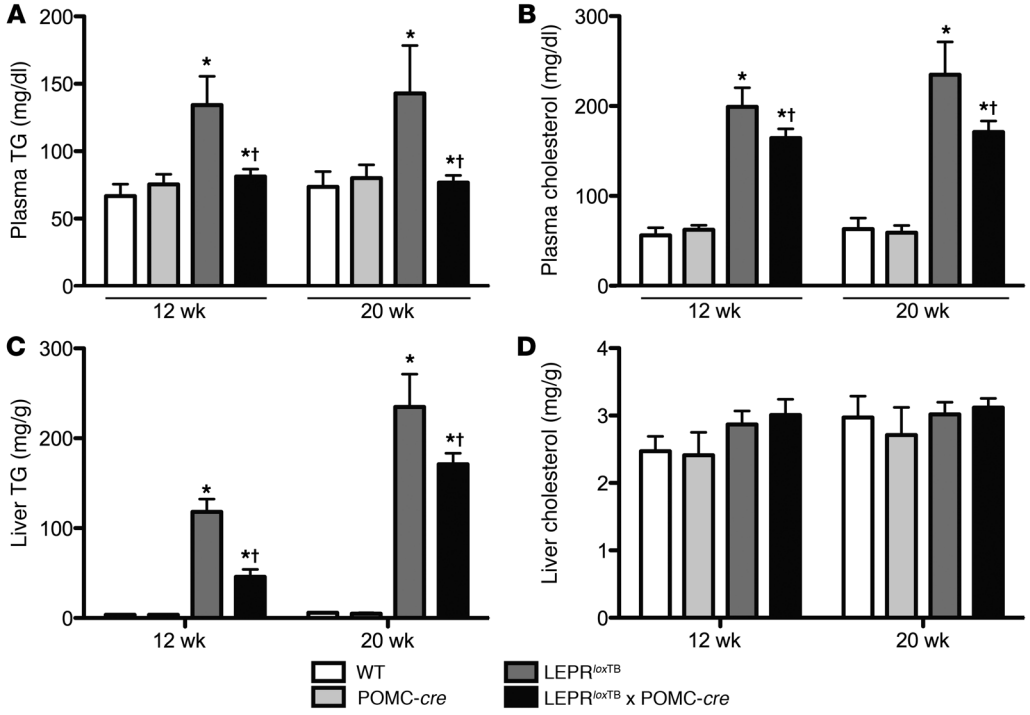

Figure 7
Selective reactivation of LEPR expression in POMC neurons improves the lipid profile. Plasma (**A** and **B**) and liver (**C** and **D**) TG and cholesterol in 12-week-old, 5-hour–fasted WT, WT expressing *Cre*-recombinase in POMC neurons, LEPR-null mice generated by inserting floxed transcription blocking sequences in the *Lepr* gene (*Lepr*^{loxTB}), and littermates in which LEPRs are selectively reactivated in POMC neurons (*Lepr*^{loxTB} × POMC-*cre*). *P < 0.05; †P < 0.05 versus WT controls and *Lepr*^{loxTB} × POMC-*cre*, respectively. n = 7–12/genotype. Data are presented as mean ± SEM.

hepatic glucose production. These findings also add to recent literature that suggests leptin may have therapeutic potential in models of type 1 and type 2 diabetes mellitus.

Methods

Animal development and care. To generate *Lepr*^{loxTB} mice, *E. coli* clones hosting BAC-containing mouse *Lepr* sequences were obtained from BACPAC (BACPAC Resources Children's Hospital Oakland, California, USA). BAC DNA clone number RP23-31K16 (containing C57BL/6J mouse strain LEPR sequences) was employed to transform EL350 bacteria (58, 59). *lox*P sequences in the backbone of the BAC plasmid were removed by homologous recombination as previously described (58, 59). Previously used and validated *lox*P-flanked transcriptional blocking sequences (23) were amplified by PCR using the following primers: 5′-CATGGGGAACAGATGCATTCCATCATGGCAATGGACCAATGATCCTCAGAGGGCTCCAGGGACACCAATTCGCGCCTAGTCGACTTCGAATAACTT-3′ and 5′-GTGTGATACCCCCCAGAATCATGAGGGAACTCAAGACCATCTATCAAATCAGACACCTCGGAGCTTTCTGGGTGGCGGCCGCTTAGTTTA-3′. They were then cloned between exons 16 and 17 of the LEPR gene by homologous recombination in EL350 (58). EL350 clones hosting correctly engineered *Lepr* BAC DNA were identified by PCR using the following primers: 5′-CAGGACATCCTGGACAGTATGCTC-3′ and 5′-CAGATGTAGCTAAAAGGCCTATCACAAACT-3′. Sequencing of these amplicons confirmed on-target homologous recombination, absence of mutations in the *lox*P-flanked transcriptional blocking sequences, and any loss of *Lepr* native sequences. The genetically engineered *Lepr* BAC DNA–targeting vector was prepared using a commercially available kit (QIAGEN). Linearized targeting vectors were electroporated into 129X1/SvJ ES cells by standard techniques at the University of Texas Southwestern Medical Center transgenic core facility. The length of homologous arms in the BAC-targeting vector precluded the use of radioactive-based Southern blot and/or long PCR assays to discriminate between ES clones hosting WT and loxP-modified *Lepr* allele. Thus, an alternative approach consisting of custom multiplex TaqMan quantitative PCR (q-PCR) analyses was devised. In this assay, we employed the commercially available MC4R assay ID Mm00457483_s1 (FAM dye-labeled probe; Applied Biosystems). This assay was used as an endogenous reference. To screen for the loxP-modified *Lepr* native allele, custom primers (5′-GGCAATGGACCAATGATCCT-3′ and 5′-GACACCTCGGAGCTTTCTGAA-3′) and VIC dye–labeled probe (5′-AGGGCTCCAGGGACA-3′) from Biosearch Technologies (Novato) were multiplexed with the MC4R assay. DNA from ES cell clones able to survive antibiotic selection was extracted as follows: ES cell medium was removed, 250 μl of extraction solution (10 mM *tris*[hydroxymethyl]aminomethane, 25 mM ethylenediaminetetraacetic acid, 0.5% sodium dodecyl sulfate, 100 mM NaCl, proteinase K 1 mg/ml, pH = 8) was added, and cells were incubated for 4 hours at 55°C. Lysates were then transferred into new tubes containing 125 μl of 5 M NaCl. Tubes were then vigorously shaken, then spun at 21,000 *g* for 10 minutes at room temperature. Supernatants were then transferred to a new tube, and an amount of 100% ethanol equal to double their volumes was added to it. Tubes were then spun at 21,000 *g* for 10 minutes at room temperature. Ethanol was then removed and DNA dissolved in distilled water. DNA was then used as template (5–100 ng) in each of the assays (primers and probes were used at 300 and 200 nM [final concentration], respectively). All assays were cycled in an Applied Biosystems PRISM 7900HT sequence detection system. We calculated the difference between the CT values of the custom and the reference q-PCRs; this was the ΔCT. Then we calculated the average WT ΔCT. Individual ΔΔCT values were calculated by subtracting the average

WT ΔCT from the individual ΔCT. ES cell clones for which ΔΔCT values were above 0.5 were deemed to be targeted. Mice were subsequently backcrossed on a C57BL/6J background for 2–3 generations. All mice were provided free access to standard chow and water and maintained on a 12-hour light/12-hour dark cycle.

Immunohistochemistry. Previously described techniques were used to visualize p-Stat3, β-endorphin, and/or ACTH immunoreactivity as well as the fluorescent reporter tdTomato in the brain or pituitary (1). Mice were fasted 24 hours and injected i.p. with leptin (5 mg/kg; Sigma-Aldrich). Mice were anesthetized 2 hours later using an i.p. injection of chloral hydrate (350 mg/kg) and then perfused transcardially with DEPC-treated 0.9% saline followed by 10% neutral buffered formalin.

Indirect calorimetry. Energy balance was assessed using TSE Metabolic Cages in the University of Texas Southwestern Mouse Phenotyping Core. Mice were acclimated for 4 days, and measurements were taken during the subsequent 4 days.

Hyperinsulinemic-euglycemic clamp. Surgical and experimental procedures were previously described (8, 60, 61). Briefly, 8- to 9-week-old mice were transferred to a sterile shoe-box–size cage lined with bedding at 9:00 am to begin a 4- to 5-hour fast. At t = –90 minutes, water was removed, and the first mouse was administered a primed, continuous infusion of [3-^{3}H]glucose (5 μCi bolus + 0.05 μCi/min). Subsequent experiments were begun at 15-minute intervals. At t = –15 and –5 minutes, blood samples from the cut tail were taken to measure insulin, glucose turnover, and 4- to 5-hour–fasted blood glucose. Glucose readings were performed using a glucometer designed for use on rodent samples. At t = 0 minutes, a continuous infusion of insulin (10 mU/kg/min; Humulin) was initiated to raise plasma insulin levels, and the infusion of [3-^{3}H]glucose was increased to 0.1 μCi/min to account for changes in specific activity. In the second cohort of mice, the insulin dose was increased to 25 mU/kg/min, and somatostatin (9 μg/kg/min) was coinfused at t = 0 minutes. In all experiments, blood samples were taken every 10 minutes thereafter to measure blood glucose. A variable GIR (50% dextrose) was used to maintain blood glucose at 150 mg/dl. Blood samples were taken every 10 minutes during the steady-state period (t = 80–120 minutes) to determine clamp hormone levels, endoR_a, and R_d.

Fast/refeeding experiments. Blood samples were taken from the cut tail at 7:30 am after a 12-hour fast to measure insulin and glucagon. One week later, food was removed again at 7:30 pm to initiate a 12-hour fast. The following morning at 7:30 am, mice were fed a carbohydrate diet; blood samples to measure fasted insulin and glucagon were taken 2 hours later.

Hormone measurements. Insulin was measured using a commercial ELISA kit in the University of Texas Southwestern Mouse Phenotyping Core. Glucagon and corticosterone were measured in the Vanderbilt University Mouse Metabolic Phenotyping Center Hormone Assay Core (Nashville, Tennessee, USA).

Pancreatic insulin and glucagon content. Pancreata were dissected from anesthetized animals, weighed, and quickly frozen in liquid nitrogen. Pancreata were then homogenized in ice-cold acid ethanol and stored overnight at 4°C. Homogenates were spun in a centrifuge the following morning, and resulting supernatants were stored at –20°C. This process was repeated twice using the remaining pellet. Supernatants were combined and warmed to 37°C; insulin and glucagon were measured using commercial radioimmunoassay kits (Millipore).

Statistics. Statistical comparisons were made using 1-way ANOVA followed by the Fisher's least significant difference test for post-hoc comparisons or t tests where appropriate. Data are presented as mean ± SEM. Statistical significance was defined as $P < 0.05$.

Study approval. The University of Texas Southwestern IACUC committee approved all procedures.

Acknowledgments

The authors would like to thank the staff of the University of Texas Southwestern Mouse Phenotyping Center for assistance. The University of Texas Southwestern Mouse Phenotyping Center is supported by NIH grants PL1 DK081182 and UL1 RR024923. This work was supported by grant 5TL1DK081181 (to E.D. Berglund) and by R01DK53301 and RL1DK081185 (to J.K. Elmquist).

Received for publication July 5, 2011, and accepted in revised form January 4, 2012.

Address correspondence to: Joel K. Elmquist, Division of Hypothalamic Research, Departments of Internal Medicine and Pharmacology, The University of Texas Southwestern Medical Center, 5323 Harry Hines Boulevard, Dallas, Texas 75390-9051, USA. Phone: 214.648.2911; Fax: 214.648.5612; E-mail: joel.elmquist@UTSouthwestern.edu.

1. Scott MM, et al. Leptin targets in the mouse brain. *J Comp Neurol*. 2009;514(5):518–532.
2. Elmquist JK, Elias CF, Saper CB. From lesions to leptin: hypothalamic control of food intake and body weight. *Neuron*. 1999;22(2):221–232.
3. Schwartz MW, Woods SC, Porte D Jr, Seeley RJ, Baskin DG. Central nervous system control of food intake. *Nature*. 2000;404(6778):661–671.
4. Flier JS, Maratos-Flier E. Lasker lauds leptin. *Cell*. 2010;143(1):9–12.
5. Fujikawa T, Chuang JC, Sakata I, Ramadori G, Coppari R. Leptin therapy improves insulin-deficient type 1 diabetes by CNS-dependent mechanisms in mice. *Proc Natl Acad Sci U S A*. 2010;107(40):17391–17396.
6. German J, et al. Hypothalamic leptin signaling regulates hepatic insulin sensitivity via a neurocircuit involving the vagus nerve. *Endocrinology*. 2009;150(10):4502–4511.
7. German JP, et al. Leptin activates a novel CNS mechanism for insulin-independent normalization of severe diabetic hyperglycemia. *Endocrinology*. 2011;152(2):394–404.
8. Hill JW, et al. Direct insulin and leptin action on pro-opiomelanocortin neurons is required for normal glucose homeostasis and fertility. *Cell Metab*. 2010;11(4):286–297.
9. Kamohara S, Burcelin R, Halaas JL, Friedman JM, Charron MJ. Acute stimulation of glucose metabolism in mice by leptin treatment. *Nature*. 1997;389(6649):374–377.
10. Pocai A, Morgan K, Buettner C, Gutierrez-Juarez R, Obici S, Rossetti L. Central leptin acutely reverses diet-induced hepatic insulin resistance. *Diabetes*. 2005;54(11):3182–3189.
11. Balthasar N, et al. Leptin receptor signaling in POMC neurons is required for normal body weight homeostasis. *Neuron*. 2004;42(6):983–991.
12. Shi H, Strader AD, Sorrell JE, Chambers JB, Woods SC, Seeley RJ. Sexually different actions of leptin in proopiomelanocortin neurons to regulate glucose homeostasis. *Am J Physiol Endocrinol Metab*. 2008;294(3):E630–E639.
13. Coppari R, et al. The hypothalamic arcuate nucleus: a key site for mediating leptin's effects on glucose homeostasis and locomotor activity. *Cell Metab*. 2005;1(1):63–72.
14. Morton GJ, et al. Leptin action in the forebrain regulates the hindbrain response to satiety signals. *J Clin Invest*. 2005;115(3):703–710.
15. Morton GJ, et al. Arcuate nucleus-specific leptin receptor gene therapy attenuates the obesity phenotype of Koletsky (fa(k)/fa(k)) rats. *Endocrinology*. 2003;144(5):2016–2024.
16. Zhang Y, et al. Pro-opiomelanocortin gene transfer to the nucleus of the solitary track but not arcuate nucleus ameliorates chronic diet-induced obesity. *NeuroScience*. 2010;169(4):1662–1671.
17. Zhang Y, et al. Simultaneous POMC gene transfer to hypothalamus and brainstem increases physical activity, lipolysis and reduces adult-onset obesity. *Eur J Neurosci*. 2011;33(8):1541–1550.
18. Huo L, et al. Leptin-dependent control of glucose balance and locomotor activity by POMC neurons. *Cell Metab*. 2009;9(6):537–547.
19. Balthasar N, et al. Divergence of melanocortin pathways in the control of food intake and energy expenditure. *Cell*. 2005;123(3):493–505.
20. Rossi J, et al. Melanocortin-4 receptors expressed by cholinergic neurons regulate energy balance and glucose homeostasis. *Cell Metab*. 2011;13(2):195–204.
21. Xu Y, et al. 5-HT2CRs expressed by pro-opiomelanocortin neurons regulate insulin sensitivity in liver. *Nat Neurosci*. 2010;13(12):1457–1459.
22. Xu Y, et al. 5-HT2CRs expressed by pro-opiomelanocortin neurons regulate energy homeostasis. *Neuron*. 2008;60(4):582–589.
23. Zigman JM, et al. Mice lacking ghrelin receptors resist the development of diet-induced obesity.

J Clin Invest. 2005;115(12):3564–3572.
24. Tartaglia LA. The leptin receptor. *J Biol Chem*. 1997;272(10):6093–6096.
25. de Vries WN, et al. Expression of Cre recombinase in mouse oocytes: a means to study maternal effect genes. *Genesis*. 2000;26(2):110–112.
26. Perez-Tilve D, et al. Melanocortin signaling in the CNS directly regulates circulating cholesterol. *Nat Neurosci*. 2010;13(7):877–882.
27. Nogueiras R, et al. The central melanocortin system directly controls peripheral lipid metabolism. *J Clin Invest*. 2007;117(11):3475–3488.
28. Shi H, Sorrell JE, Clegg DJ, Woods SC, Seeley RJ. The roles of leptin receptors on POMC neurons in the regulation of sex-specific energy homeostasis. *Physiol Behav*. 2010;100(2):165–172.
29. Williams KW, et al. Segregation of acute leptin and insulin effects in distinct populations of arcuate proopiomelanocortin neurons. *J Neurosci*. 2010; 30(7):2472–2479.
30. Wasserman DH. Four grams of glucose. *Am J Physiol Endocrinol Metab*. 2009;296(1):E11–E21.
31. Wang MY, et al. Leptin therapy in insulin-deficient type I diabetes. *Proc Natl Acad Sci U S A*. 2010; 107(11):4813–4819.
32. Liang Y, et al. Reduction in glucagon receptor expression by an antisense oligonucleotide ameliorates diabetic syndrome in db/db mice. *Diabetes*. 2004;53(2):410–417.
33. Sloop KW, et al. Hepatic and glucagon-like peptide-1-mediated reversal of diabetes by glucagon receptor antisense oligonucleotide inhibitors. *J Clin Invest*. 2004;113(11):1571–1581.
34. Liu L, et al. Intracerebroventricular leptin regulates hepatic but not peripheral glucose fluxes. *J Biol Chem*. 1998;273(47):31160–31167.
35. Rossetti L, et al. Short term effects of leptin on hepatic gluconeogenesis and in vivo insulin action. *J Biol Chem*. 1997;272(44):27758–27763.
36. Li X, Wu X, Camacho R, Schwartz GJ, LeRoith D. Intracerebroventricular leptin infusion improves glucose homeostasis in lean type 2 diabetic MKR mice via hepatic vagal and non-vagal mechanisms. *PLoS One*. 2011;6(2):e17058.
37. Shi ZQ, Nelson A, Whitcomb L, Wang J, Cohen AM. Intracerebroventricular administration of leptin markedly enhances insulin sensitivity and systemic glucose utilization in conscious rats. *Metabolism*. 1998;47(10):1274–1280.
38. Minokoshi Y, Haque MS, Shimazu T. Microinjection of leptin into the ventromedial hypothalamus increases glucose uptake in peripheral tissues in rats. *Diabetes*. 1999;48(2):287–291.
39. Babic T, Purpera MN, Banfield BW, Berthoud HR, Morrison CD. Innervation of skeletal muscle by leptin receptor-containing neurons. *Brain Res*. 2010;1345:146–155.
40. Silver DL, Jiang XC, Tall AR. Increased high density lipoprotein (HDL), defective hepatic catabolism of ApoA-I and ApoA-II, and decreased ApoA-I mRNA in ob/ob mice. Possible role of leptin in stimulation of HDL turnover. *J Biol Chem*. 1999;274(7):4140–4146.
41. Silver DL, Wang N, Tall AR. Defective HDL particle uptake in ob/ob hepatocytes causes decreased recycling, degradation, and selective lipid uptake. *J Clin Invest*. 2000;105(2):151–159.
42. Wiegman CH, et al. Hepatic VLDL production in ob/ob mice is not stimulated by massive de novo lipogenesis but is less sensitive to the suppressive effects of insulin. *Diabetes*. 2003;52(5):1081–1089.
43. Donahoo WT, Stob NR, Ammon S, Levin N, Eckel RH. Leptin increases skeletal muscle lipoprotein lipase and postprandial lipid metabolism in mice. *Metabolism*. 2011;60(3):438–443.
44. Prieur X, Tung YC, Griffin JL, Farooqi IS, O'Rahilly S, Coll AP. Leptin regulates peripheral lipid metabolism primarily through central effects on food intake. *Endocrinology*. 2008;149(11):5432–5439.
45. Sharma A, et al. Hepatic gene expression profiling reveals key pathways involved in leptin-mediated weight loss in ob/ob mice. *PLoS One*. 2010; 5(8):e12147.
46. Samuel VT, et al. Mechanism of hepatic insulin resistance in non-alcoholic fatty liver disease. *J Biol Chem*. 2004;279(31):32345–32353.
47. Seppala-Lindroos A, et al. Fat accumulation in the liver is associated with defects in insulin suppression of glucose production and serum free fatty acids independent of obesity in normal men. *J Clin Endocrinol Metab*. 2002;87(7):3023–3028.
48. Marchesini G, et al. Association of nonalcoholic fatty liver disease with insulin resistance. *Am J Med*. 1999;107(5):450–455.
49. Schonfeld G, Yue P, Lin X, Chen Z. Fatty liver and insulin resistance: not always linked. *Trans Am Clin Climatol Assoc*. 2008;119:217–223.
50. Raubenheimer PJ, Nyirenda MJ, Walker BR. A choline-deficient diet exacerbates fatty liver but attenuates insulin resistance and glucose intolerance in mice fed a high-fat diet. *Diabetes*. 2006;55(7):2015–2020.
51. Harlan SM, et al. Ablation of the leptin receptor in the hypothalamic arcuate nucleus abrogates leptin-induced sympathetic activation. *Circ Res*. 2011;108(7):808–812.
52. Park S, Ahn IS, Kim da S. Central infusion of leptin improves insulin resistance and suppresses beta-cell function, but not beta-cell mass, primarily through the sympathetic nervous system in a type 2 diabetic rat model. *Life Sci*. 2010;86(23–24):854–862.
53. Haque MS, Minokoshi Y, Hamai M, Iwai M, Horiuchi M, Shimazu T. Role of the sympathetic nervous system and insulin in enhancing glucose uptake in peripheral tissues after intrahypothalamic injection of leptin in rats. *Diabetes*. 1999;48(9):1706–1712.
54. Pocai A, Obici S, Schwartz GJ, Rossetti L. A brain-liver circuit regulates glucose homeostasis. *Cell Metab*. 2005;1(1):53–61.
55. Luquet S, Perez FA, Hnasko TS, Palmiter RD. NPY/AgRP neurons are essential for feeding in adult mice but can be ablated in neonates. *Science*. 2005;310(5748):683–685.
56. Padilla SL, Carmody JS, Zeltser LM. Pomc-expressing progenitors give rise to antagonistic neuronal populations in hypothalamic feeding circuits. *Nat Med*. 2010;16(4):403–405.
57. Myers MG Jr, Munzberg H, Leinninger GM, Leshan RL. The geometry of leptin action in the brain: more complicated than a simple ARC. *Cell Metab*. 2009;9(2):117–123.
58. Lee EC, et al. A highly efficient Escherichia coli-based chromosome engineering system adapted for recombinogenic targeting and subcloning of BAC DNA. *Genomics*. 2001;73(1):56–65.
59. Liu P, Jenkins NA, Copeland NG. A highly efficient recombineering-based method for generating conditional knockout mutations. *Genome Res*. 2003;13(3):476–484.
60. Berglund ED, et al. Fibroblast growth factor 21 controls glycemia via regulation of hepatic glucose flux and insulin sensitivity. *Endocrinology*. 2009;150(9):4084–4093.
61. Berglund ED, et al. Glucose metabolism in vivo in four commonly used inbred mouse strains. *Diabetes*. 2008;57(7):1790–1799.